FRISP Report No. 17 (2006)

The impact of mixing parameterisation and bathymetry filtering on the simulated hydrography along steep continental shelf regions in terrain following ocean models

***Malte Thoma*[1,2], *Klaus Grosfeld*[3,4], *Manfred A. Lange*[1]**
(1) Institute for Geophysics, University of Münster, Germany
(2) now at: British Antarctic Survey, Cambridge, United Kingdom
(3) Department of Physics/MARUM, University of Bremen, Germany
(4) Alfred Wegener Institute for Polar and Marine Research, Bremerhaven, Germany

Introduction

General vertical coordinates in ocean models can be parameterised in three different ways: The most straightforward and mathematical easiest method are geopotential surfaces, where vertical coordinates are parallel to one another and perpendicular to the earth's radius. One example for this type of ocean models is the Modular Ocean Model (MOM) (e.g., Bryan & Cox, 1968; Cox, 1984; Haidvogel & Beckmann, 1999; Griffies *et al.*, 2003). One disadvantage of this $z-$coordinate type models is that several nodes (and therefore computational costs) are wasted if processes in the deep ocean and on shallow shelves are investigated. This type of ocean models is also not able to simulate overflow process adequately without additional empirical bottom boundary layer mixing schemes (e.g., Beckmann & Döscher, 1997; Ezer & Mellor, 2004).
The perhaps most natural vertical coordinate system is an isopycnal one, where the surfaces are orientated along constant densities. No spurious diapycnal mixing occurs in this type of model, but the vertical coordinates are adaptive and must be recalculated each timestep. In addition, a special treatment of surface and bottom boundary layers is necessary, leading to additional complexity and computational costs. The most common isopycnic ocean model is the Miami Isopycnic Model (MICOM) (e.g., Bleck, 1978; Haidvogel & Beckmann, 1999).
The third type of ocean models uses terrain following coordinates. These $\sigma-$coordinate models are most convenient to represent the bottom topography. So far they are mainly used in high resolution regional models where the pressure gradient error, associated with this type of models (e.g., Haney, 1991) is probably of minor importance (Ezer *et al.*, 2002). Models using terrain following coordinates are the Princton Ocean Model (POM) (Blumberg & Mellor, 1987), the s-coordinate primitive equation model (SPEM) (Haidvogel *et al.*, 1991) and Rombax (Thoma *et al.*, 2005b).

In this study we analyse two different aspects of ocean modelling with the terrain following coordinate model Rombax:

- the impact of different mixing schemes and
- the impact of the bathymetry

on the hydrography and the basal mass balance at the ice shelf – ocean interface in the vicinity of steep continental slopes. In our study we focus on the Eastern Weddell Ice

Shelf (EWIS) region, because of its narrow continental shelf and its importance for the preconditioning of water masses in the southern Weddell Sea.

Mixing schemes

In previous versions of Rombax (Grosfeld *et al.*, 1997) a simple Laplacian mixing scheme was used for the diffusion of momentum and tracer (Mellor & Blumberg, 1985; Gerdes, 1993). As unwanted diapycnal mixing naturally occurs along $\sigma-$coordinates, we implemented the implicit flux-corrected transport (FCT) scheme for tracers (i.e., temperature and salinity). The diapycnal mixing of momentum along terrain-following-coordinate surfaces is reduced by local and adaptive eddy coefficients. For this calculation a Smagorinsky type algorithm is used, considering the local tension, shear stress and grid-cell size (e.g., Smagorinsky, 1963; Haidvogel & Beckmann, 1999; Griffies, 2004). Vertical mixing depends on the stability of the water column. Therefore we apply a locally defined Richardson Number dependent scheme after Pacanowski & Philander (1981). Timmermann & Beckmann (2004) showed that this scheme is suitable for the Weddell Sea, applying an additional background viscosity in the topmost ocean layer due to the sea ice coverage.

Filtering the bathymetry

In general, bathymetry representation as close as possible to nature is expected to give the most realistic results for modelling the oceanic flow regime. But for two numerical reasons filtering (i.e., smoothing) of the bathymetry may be necessary. First of all, steep slopes in association with a fine horizontal model resolution may lead to numerical instabilities. Second, according to Mellor & Blumberg (1985) unwanted diapycnal mixing introduced by a Laplacian diffusion scheme surpasses tolerable limits in terrain following ocean models if the angle between the σ-surfaces and the horizontal plane (which depends on the grid cell size) exceeds about 10%. Therefore, a filter is defined by four parameters:

1. the *(sub-)region* of the model domain where the filter is applied,
2. the *area* or range of surrounding nodes included for the recalculation of the new bathymetry value,
3. the *shape* or weighting of the adjacent nodes, and
4. the *limit*.

The limit yields the lower bound from which the filtering sets in if the ocean bottom slope exceeds this specific limit. For example, a limit of 0% leads to a filtering of all nodes inside the selected region while a limit of 8% induces filtering only when the gradient of the bathymetry exceeds this value. In this study one filter is applied to the total model domain. Figure 1 shows the area and shape of different filters used in this study.

Model set-up

If not explicitly mentioned, the used ocean model setup is identical to the model described by Thoma *et al.* (2005a,b). We choose the eastern Weddell Sea as test region for this

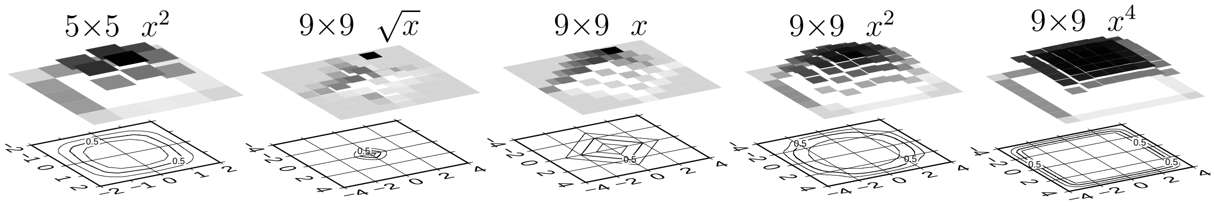

Figure 1: Area and shape of used filter types (see also Table 1).

study. A steep bathymetry (Figure 2) ensures discernible filter effects, and the interaction with the Eastern Weddell Ice Shelves allows the calculated basal mass balance to be used as a comparative value between different model configurations. The prescribed vertically integrated stream function at the northern and eastern model boundaries ensures a reasonable flow pattern (Figure 3) in this regional model. The hydrography taken from Gouretski *et al.* (1999) is used to initialise the ocean model as well as for the restoring at lateral open boundaries. At the ocean surface a climatological wind stress field after Kottmeier & Sellmann (1996) is applied, while tracers of the uppermost ocean layer are restored to 1.9°C (temperature) and 34.5 (salinity) with a restoring timescale of 10 days.

Table 1 specifies the used models in three paragraphs. In the first paragraph the model setups differ from one another by the parameterisation of diffusion and by the vertical resolution. If not marked with a (√) Laplacian diffusion with constant eddy coefficients is applied for the diffusion of tracer and momentum (horizontal: $100\,\mathrm{m^2s^{-1}}$ and $400\,\mathrm{m^2s^{-1}}$;

Model	FCT[1]	Smag[2]	Rich[3]	σ[4]	Filter[5] area	shape	limit[6]	basal mass balance ($\mathrm{m\,y^{-1}}$)	fresh water flux (mSv)	Δ[7]
$^{14}\mathcal{M}$				10				0.941	1.97	6.9%
$^{14}\mathcal{M}^{\mathcal{F}}$	√			10				0.825	1.73	−6.2%
$^{14}\mathcal{M}^{\mathcal{FSR}}$	√	√	√	10				0.895	1.88	1.7%
$^{19}\mathcal{M}^{\mathcal{FSR}}$	√	√	√	15				0.880	1.85	–
$^{19}\mathcal{M}^{\mathcal{FSR}}_{5x^28}$	√	√	√	15	5×5	x^2	8% (1%)	0.907	1.90	3.1%
$^{19}\mathcal{M}^{\mathcal{FSR}}_{5x^24}$	√	√	√	15	5×5	x^2	4% (9%)	1.008	2.12	14.6%
$^{19}\mathcal{M}^{\mathcal{FSR}}_{5x^22}$	√	√	√	15	5×5	x^2	2% (20%)	1.078	2.26	22.5%
$^{19}\mathcal{M}^{\mathcal{FSR}}_{5x^20}$	√	√	√	15	5×5	x^2	0% (100%)	1.108	2.32	25.9%
$^{19}\mathcal{M}^{\mathcal{FSR}}_{9\sqrt{x}4}$	√	√	√	15	9×9	$\sqrt{x}$	4% (9%)	0.933	1.96	6.0%
$^{19}\mathcal{M}^{\mathcal{FSR}}_{9x4}$	√	√	√	15	9×9	x	4% (9%)	1.040	2.18	18.3%
$^{19}\mathcal{M}^{\mathcal{FSR}}_{9x^24}$	√	√	√	15	9×9	x^2	4% (9%)	1.098	2.31	24.9%
$^{19}\mathcal{M}^{\mathcal{FSR}}_{9x^44}$	√	√	√	15	9×9	x^4	4% (9%)	1.115	2.34	26.8%

Table 1: Overview of model experiments performed in this study.
[1] Flux-Corrected Transport.
[2] Smagorinsky type horizontal diffusion of momentum.
[3] Richardson Number dependent vertical diffusion of momentum.
[4] The given number of $\sigma-$layers are complemented by four equidistant $z-$layers in the topmost 180 m of the open ocean.
[5] The filter-*region* is always the total model domain.
[6] The number in brackets describes the percentage of the totally filtered number of nodes.
[7] Deviation of the calculated basal mass balance with respect to the control model $^{19}\mathcal{M}^{\mathcal{FSR}}$.

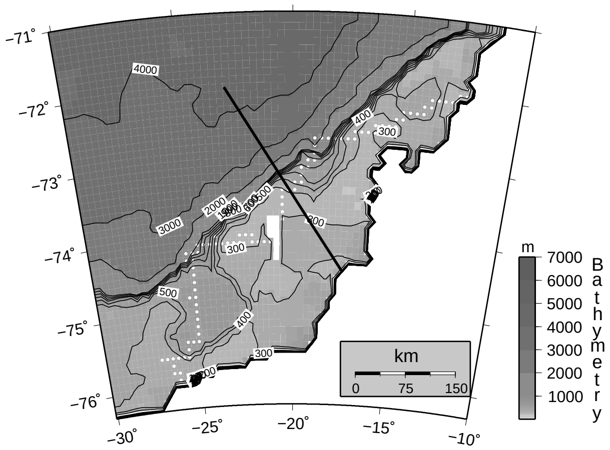

Figure 2: Bathymetry of the model region. White circles mark the ice shelf edge. The black line indicates the cross section where model results are compared.

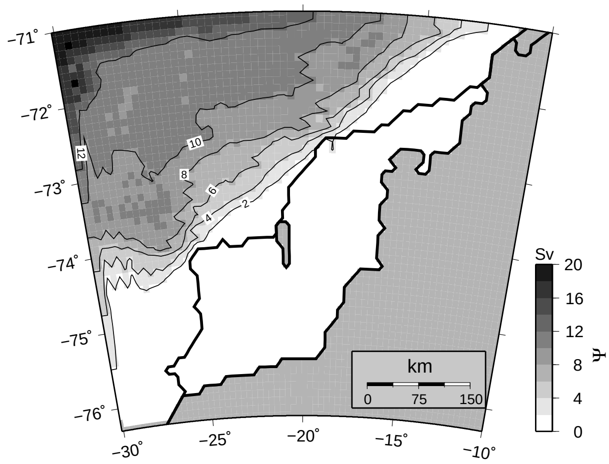

Figure 3: Annual mean of the vertical integrated mass transport in the Eastern Weddell Sea for the control model ${}^{19}\mathcal{M}^{\mathcal{FSR}}$ after 15 years of integration.

vertical: $0.05\times10^{-3}\,\mathrm{m^2s^{-1}}$ and $0.80\times10^{-3}\,\mathrm{m^2s^{-1}}$), respectively. The models in the second paragraph differ by the number of filtered nodes as given by the depth gradient of the bathymetry, while the shape of the filter is modified for the models in the third paragraph.

Results and discussion

Due to the limited model domain of about 68×54 nodes (covering a region of about 500×600 km) a quasi steady state of the model is already reached after about 5 years. However, all model experiments are integrated for at least 15 years to get stable results. The shown results represent means between the years 5 and 15 of the integration. The basal mass balance given in Table 1 is calculated with the three-equation formulation (Holland & Jenkins, 1999), considering heat and salt conservation at the ice-ocean interface. To compare the impact of different model configurations on the hydrography, we limit ourself to one single temperature cross section along the track given in Figure 2. In the following subsection we discuss the impact of different mixing schemes, subsequently the impact of different filter operators are studied.

The impact of various mixing schemes

The configuration of the model experiments discussed in this section are listed in the first paragraph of Table 1. These experiments differ from each other by the used mixing schemes (${}^{14}\mathcal{M}$, ${}^{14}\mathcal{M}^{\mathcal{F}}$, and ${}^{14}\mathcal{M}^{\mathcal{FSR}}$) as well as the number of vertical layers (${}^{14}\mathcal{M}^{\mathcal{FSR}}$ and ${}^{19}\mathcal{M}^{\mathcal{FSR}}$). The impact of different mixing schemes on the simulated hydrography is shown in Figure 4. The most conspicuous feature is the very week developed WDW core in experiment ${}^{14}\mathcal{M}$, where constant diffusivities are used for tracer and momentum (Figure 4a). The temperature maximum of the WDW is more than about 150 km apart from the continental shelf break and is notedly below 0.5°C. Compared with field measurements (e.g., Fahrbach *et al.*, 1994; Heywood *et al.*, 1998) all other experiments, using the implicit FCT scheme for the tracer diffusion, give much better results: The maximum temperature of the WDW is in about 100 km distance to the continental shelf break and the temperature is notedly higher in this area. The largest impact on the temperature cross section has the implicit FCT scheme for the tracer diffusion ($^{14}\mathcal{M}^{\mathcal{F}}$, Figure 4b). Here the explicit tracer diffusion of $^{14}\mathcal{M}$, with constant tracer diffusivities is replaced with the implicit FCT scheme, based upon the idea to find locally a minimum mixing that is consistent with thermodynamical constraints (Gerdes, 1991). This model has the highest WDW core temperature of about 0.8°C. The adaptive diffusion schemes for the momentum ($^{14}\mathcal{M}^{\mathcal{FSR}}$, Figure 4c) reduce the maximum temperature, with respect to experiment $^{14}\mathcal{M}^{\mathcal{F}}$, and reduces the distance between the 0°C

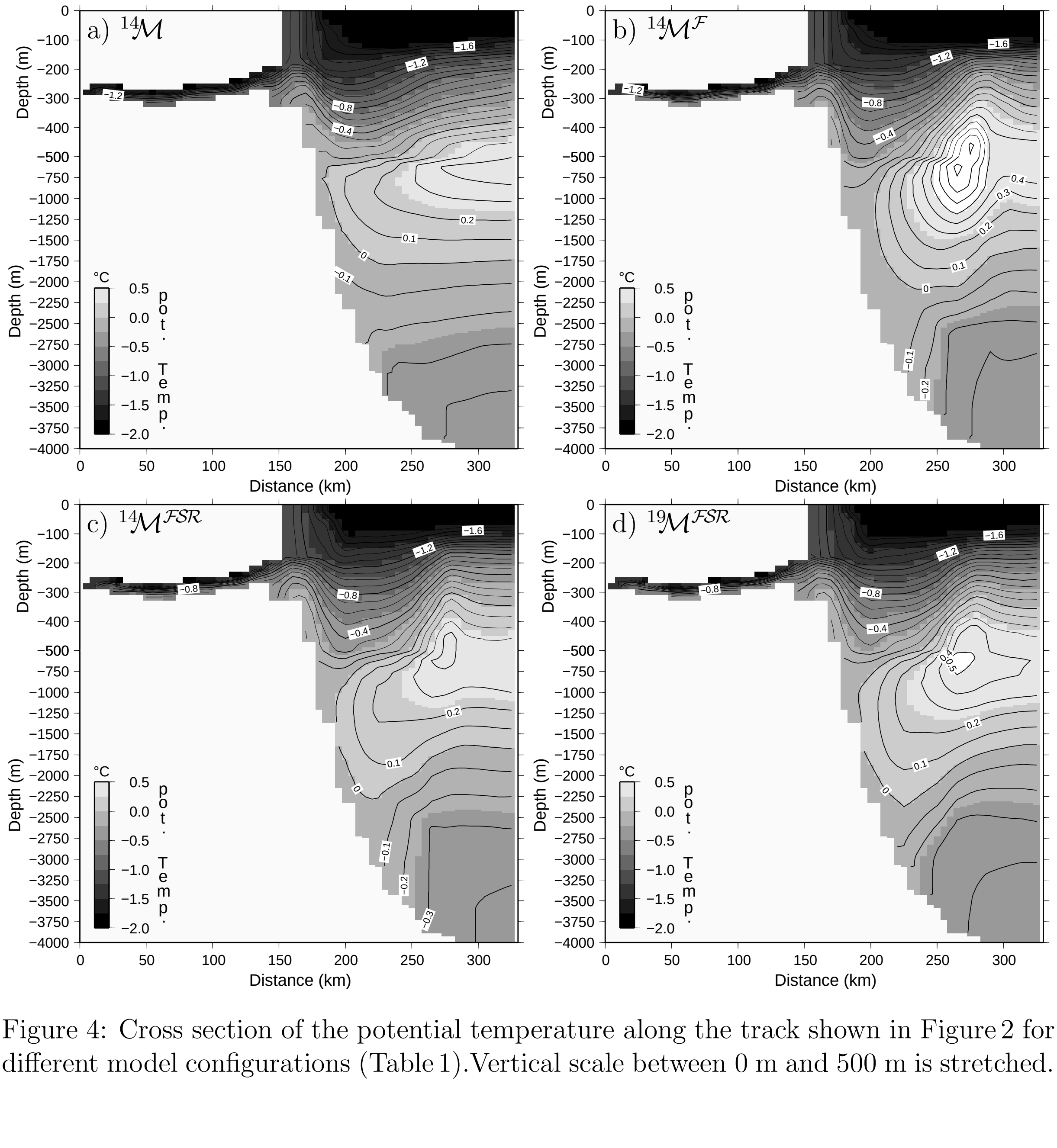

Figure 4: Cross section of the potential temperature along the track shown in Figure 2 for different model configurations (Table 1).Vertical scale between 0 m and 500 m is stretched.

isotherm (which is defined as the lower bound for the WDW, e.g., Grosfeld *et al.*, 2001) and the continental shelf break, too. If the vertical resolution of the model is increased ($^{19}\mathcal{M}^{\mathcal{FSR}}$, Figure 4d), the core temperature of the WDW rises again above 0.5°C. Furthermore, the artificial deviation of the −0.1, −0.2, and −0.3°C isotherms near the continental shelf break in about 3000 m depth is reduced. The mean horizontal eddy diffusivity for momentum, calculated with the Smagorinsky scheme, for experiments $^{14}\mathcal{M}^{\mathcal{FSR}}$ and $^{19}\mathcal{M}^{\mathcal{FSR}}$ is about $18.3\,\mathrm{ms}^{-1}$, but peaks of about $260\,\mathrm{ms}^{-1}$ are reached, especially in the vicinity of the ice shelf margin (not shown). The mean Richardson Number dependent vertical eddy diffusion coefficient is about $0.44\times10^{-3}\,\mathrm{ms}^{-1}$ for experiment $^{14}\mathcal{M}^{\mathcal{FSR}}$ and about $0.39\times10^{-3}\,\mathrm{ms}^{-1}$ for experiment $^{19}\mathcal{M}^{\mathcal{FSR}}$, where the intervals between the $\sigma-$layers are smaller. These values replace the constant diffusivities ($400\,\mathrm{ms}^{-1}$ horizontal, $0.80\times10^{-3}\,\mathrm{ms}^{-1}$ vertical) used in experiments $^{14}\mathcal{M}$ and $^{14}\mathcal{M}^{\mathcal{F}}$.

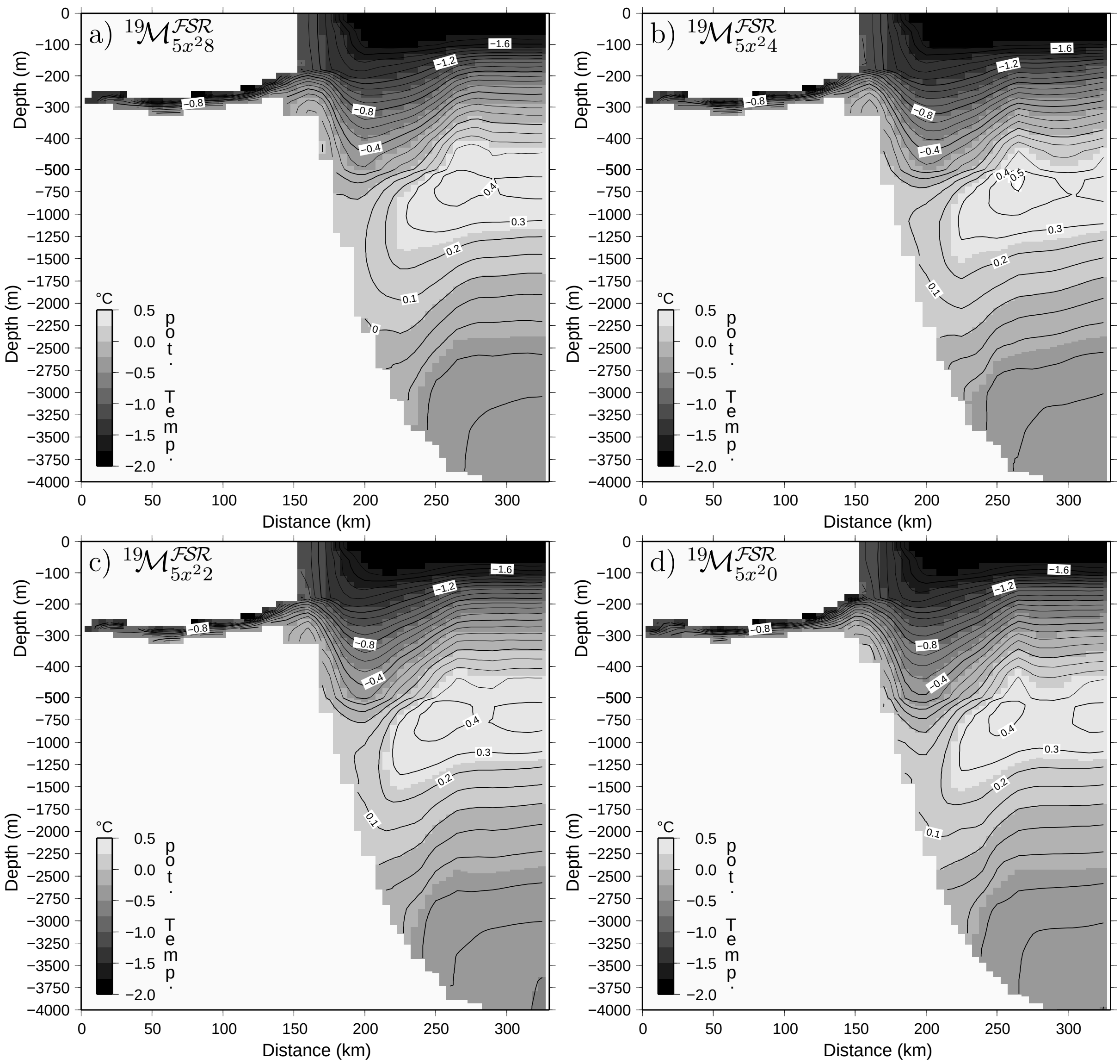

Figure 5: As Figure 4, but for model configurations differing by the number of filtered nodes (Table 1).

Impact of different bathymetry filter types

Comparing the cross sections in Figure 5 with the control experiment ${}^{19}\mathcal{M}^{\mathcal{FSR}}$ (Figure 4d) the impact of the number of filtered nodes becomes obvious: The more nodes are filtered (and hence the smoother the bathymetry is), the closer the WDW sets to the smoothed continental shelf break. While the 0°C isotherm just touches the shelf break in about 1500 m depth for ${}^{19}\mathcal{M}^{\mathcal{FSR}}$, even a poor filtering of 1% of the total numer of nodes (${}^{19}\mathcal{M}^{\mathcal{FSR}}_{5x^28}$, Figure 5a) makes sure that from about 750 m to about 2200 m the temperature at the shelf break surpasses 0°C. If all nodes are filtered (${}^{19}\mathcal{M}^{\mathcal{FSR}}_{5x^20}$, Figure 5d) even the 0.1°C isotherm touches the shelf break between about 1000 m and 2200 m depth. The maximum temperature of the WDW core varies around 0.5°C in all model experiments, reaching a maximum in ${}^{19}\mathcal{M}^{\mathcal{FSR}}_{5x^24}$, where 9% of all nodes are filtered. The last column in Table 1 shows that basal melting in the ice shelf cavity of the EWIS region increases with the

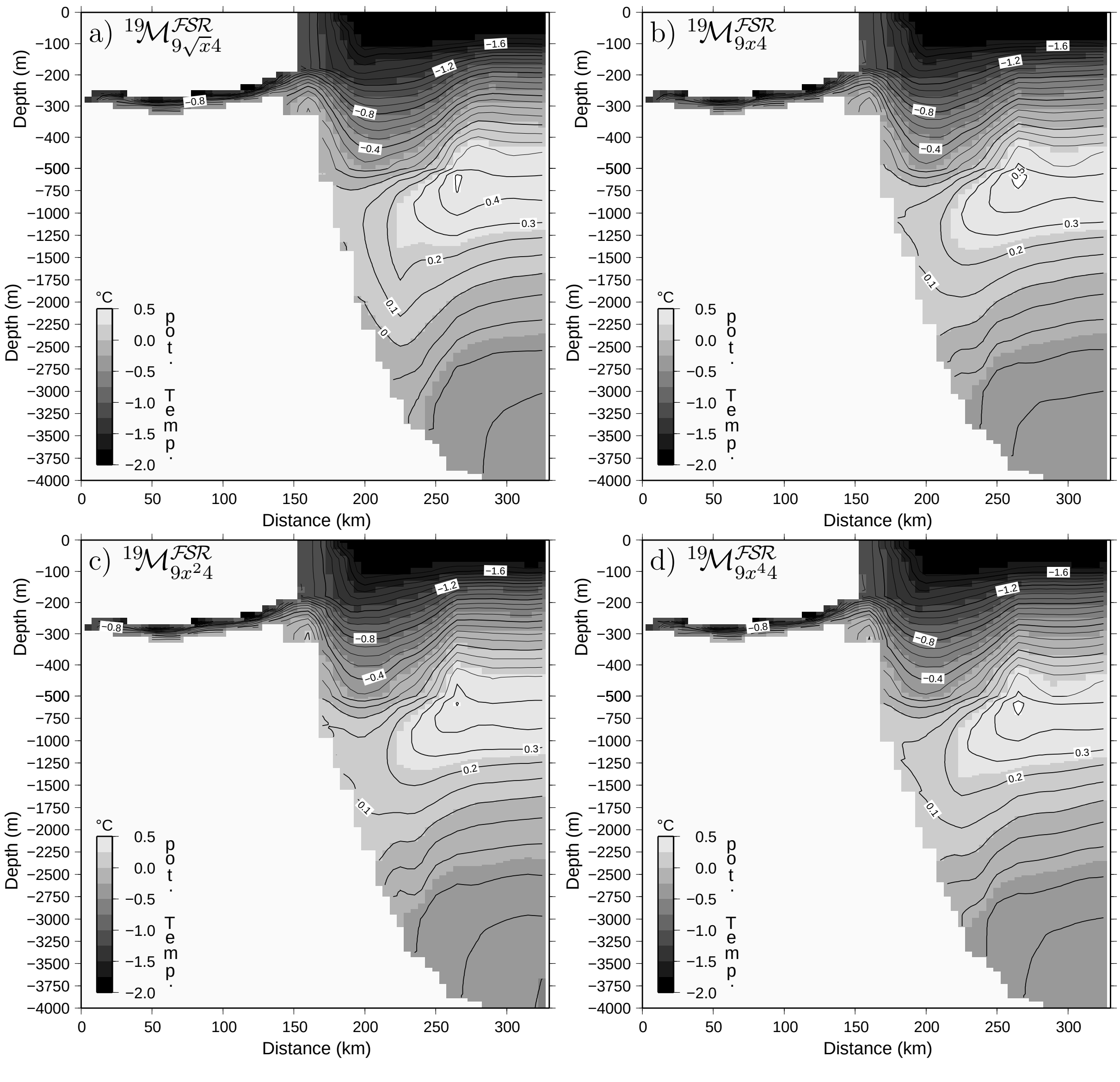

Figure 6: As Figure 4, but for model configurations differing by the filter shape (Table 1).

number of filtered nodes. As a possible explanation for this we suggest that a smoother continental shelf break allows warmer water from the deeper ocean to flood the cavity and therefore increases the ocean temperature at the ice shelf base. Comparing the results for experiments with various filter shapes and sizes (area of filter) (${}^{19}\mathcal{M}^{\mathcal{FSR}}_{5x^24}$, Figure 5b and ${}^{19}\mathcal{M}^{\mathcal{FSR}}_{9x^24}$, Figure 6c) the same observations as before are valid: The larger the area is where the filter is applied (5×5 or 9×9 for experiments ${}^{19}\mathcal{M}^{\mathcal{FSR}}_{5x^24}$ and ${}^{19}\mathcal{M}^{\mathcal{FSR}}_{9x^24}$) the more melting takes place (24.9% instead of 14.6%, Table 1) and a WDW core closer to the shelf break (see 0.1°C isotherm). Contemporaneously the temperature of the WDW core is reduced.

The impact of different filter shapes (Figure 6) on the basal mass balance is similar to the impact of the number of filtered nodes: The more the filter operator smooths the bathymetry the more warmer waters enters the cavity and the more fresh water is produced. While the position of the WDW core does not change, if the filter shape or area is modified (Figure 6a-d and Figure 5c), a minor change in the temperature just before the shelf break can be observed.

Summary and conclusion

This study aims to show different aspects of ocean model parameterisation when simulating processes along the continental shelf margin in the Southern Ocean. Because of vast narrow shelf regions, the Antarctic coastal current sets close to the ice shelves bringing WDW or its derivative Modified WDW (MWDW) into contact with the ice shelves. The available heat leads to high melt rates underneath the ice shelves, influencing significantly the freshwater budget of the Weddell Sea (Jacobs *et al.*, 1992; Timmermann *et al.*, 2001; Hellmer, 2004). Hence, the calculated freshwater formation rate in ocean models, which are able to simulate ocean circulation in ice shelf cavities, depends on the one hand strongly on the representation of the bathymetry and ice shelf geometry in that region (Grosfeld *et al.*, 1997; Nicolaus & Grosfeld, 2002). On the other hand, the parameterisation of model physics determines how the hydrography is represented in the model and hence, the available heat for ice shelf melting in the cavity.

In our study we have demonstrated particularly,

- that the choice of the implicit FCT diffusion scheme outclasses a simple explicit Laplacian diffusion scheme in simulating the coastal current,
- that adjustable momentum diffusion schemes, like the Smagorinsky (1963) and Pacanowski & Philander (1981) schemes, reduce the temperature of the WDW core but admit a closer distance between the WDW and the continental shelf break,
- that a moderate increase of the vertical resolution (19 instead of 14 layers) significantly improves the model results,
- that filtering of the bathymetry, in particular of steep continental shelf breaks, increases the penetration of warmer water masses into ice shelf cavities, leading to an increased freshwater formation of up to 25% (strongly depending on the used filter operator). On the other hand insufficient knowledge of the real bathymetry may permit weak smoothing if thereby the observed hydrography can be better reproduced.

We conclude, that Laplacian tracer-diffusion is unsuitable for modelling ice-shelf ocean interaction in regions with only a narrow (or negligible) continental shelf. Adaptive momentum diffusion coefficients reduce the strong impact of the FCT scheme on the WDW. Furthermore we suggest, that a suitable number of vertical layers is necessary for the modelling of shelf processes, especially if both, the deep ocean and a shallow continental shelf are included in the model domain. If hydrographic observations are compared with model simulations, cautious topography filtering may improve the results, but attention has to be payed not to overreach. From this study we recommend a spatial filtering with a quadratic filter weight (x^2) if the gradient limit exceeds 4%, considering 5×5 nodes at the most (first filter operator in Figure 1). Summarising we conclude, that the implemented momentum mixing schemes together with the implicit FCT scheme and a moderate filtering of the gridded bathymetry yield an improved (compared to, e.g., Thoma *et al.*, 2005b) and reasonable (compared to observations, e.g., Fahrbach *et al.*, 1994; Heywood *et al.*, 1998) simulation of the hydrography in the EWIS region, which can be base for further studies of ice shelf – ocean interaction processes in the southern Weddell Sea.

Acknowledgements: This work is part of the German CLIVAR/marin-project. Funding by the Bundesministerium für Bildung, Wissenschaft, Forschung und Technologie (bmb+f) der Bundesrepublik Deutschland, contract 03F0377C, is gratefully acknowledged. The authors are grateful to Rüdiger Gerdes for providing the numerical FCT-code in σ-coordinates.

References

Beckmann, A. & Döscher, R. 1997. A method for improved representation of dense water spreading over topography in geopotential-coordinate models, *Journal of Physical Oceanography*, *27*, 581–591.

Bleck, R. 1978. Finite difference equations in generalized vertical coordinates. part I: Total energy conservation, *Beitrge zur Physik der Atmosphre*, *51*, 360–372.

Blumberg, A. F. & Mellor, G. L. 1987. A description of a three-dimensional coastal ocean circulation model, in *Three-Dimensional Coastal Ocean Models, Coastal Estuarine Studies*, edited by N. S. Heaps, vol. 4, pp. 1–16, American Geophysical Union, Washington.

Bryan, K. & Cox, M. D. 1968. A nonlinear model of an ocean driven by wind and differential heating: Part i. description of the three-dimensional velocity and density fields, *Journal of the Atmospheric Sciences*, *25*.

Cox, M. D. 1984. A primitive equation, 3-dimensional model of the ocean, *GFDL Ocean Group Technical Report No. 1*, Princeton University.

Ezer, T. & Mellor, G. L. 2004. A generalized coordinate ocean model and a comparison of the bottom boundary layer dynamics in terrain-following and in z-level grids, *Ocean Modelling*, *6*, 379–403.

Ezer, T., Arango, H. & Shchepetkin, A. F. 2002. Developments in terrain-following ocean models: intercomparisons of numerical aspects, *Ocean Modelling*, *4*, 249–267.

Fahrbach, E., Peterson, R. G., Rohardt, G., Schlosser, P. & Bayer, R. 1994. Suppression of bottom water formation in the southeastern Weddell Sea, *Deep-Sea Research*, *41*, 389–411.

Gerdes, R. 1991. The influence of numerical advection schemes on the result of ocean general circulation models, *Climate Dynamics*, *5*, 211–226.

Gerdes, R. 1993. A primitive equation ocean circulation model using a general vertical transformation. Part 1: Description and testing of the model, *Journal of Geophysical Research*, *98*, 14,683–14,701.

Gouretski, V., Jancke, K., Reid, J., Swift, J., Rhines, P., Schlitzer, R. & Yashayaev, I. 1999. WOCE Hydrographic Programme Special Analysis Centre, Atlas of Ocean Sections, CD-ROM.

Griffies, S. M., 2004. *Fundamentals of ocean climate models*, Princeton University Press, Princeton.

Griffies, S. M., Harrison, R. C., M. J. Pacanowski & Rosati, A., 2003. *A Technical Guide to MOM4*, NOAA/Geophysical Fluid Dynamics Laboratory, Princton.

Grosfeld, K., Gerdes, R. & Determann, J. 1997. Thermohaline circulation and interaction beneath ice shelf cavities and the adjacent open ocean, *Journal of Geophysical Research*, *102*, 15,595–15,610.

GROSFELD, K., SCHRÖDER, M., FAHRBACH, E., GERDES, R. & MACKENSEN, A. 2001. How iceberg calving and grounding change the circulation and hydrography in the Filchner Ice Shelf - ocean system, *Journal of Geophysical Research*, *106*, 9039–9055.

HAIDVOGEL, D. B. & BECKMANN, A., 1999. *Numerical ocean circulation modeling*, Imperial Collage Press, London.

HAIDVOGEL, D. B., WILKIN, J. L. & YOUNG, R. 1991. A semi-spectral primitive equation ocean circulation model using vertical sigma and orthogonal curvilinear horizontal coordinates, *Journal of Computational Physics*, *94*, 151–185.

HANEY, R. L. 1991. On the pressure gradient force over steep topog- raphy in sigma coordinate models, *Journal of Physical Oceanography*, *21*, 610–619.

HELLMER, H. H. 2004. Impact of Antarctic ice shelf basal melting on sea ice and deep ocean properties, *Geophysical Research Letters*, *31*, 1–4, L10307, doi:10.1029/2004GL019506.

HEYWOOD, K. J., LOCARNINI, R. A., FREW, R. D., DENNIS, P. F. & KING, B. A. 1998. Transport and water masses of the Antarctic slope front system in the eastern Weddell Sea, in *Ocean, Ice, and Atmosphere: Interactions at the Antarctic Continental Margin*, edited by S. S. Jacobs & R. F. Weiss, vol. 75 of *Antarctic Research Series*, pp. 203–214, Americal Geophysical Union, Washington, D.C.

HOLLAND, D. M. & JENKINS, A. 1999. Modeling thermodynamic ice-ocean interaction at the base of an ice shelf, *Journal of Physical Oceanography*, *29*, 1787–1800.

JACOBS, S. S., HELLMER, H. H., DOAKE, C. S. M., JENKINS, A. & FROLICH, R. M. 1992. Melting of ice shelves and mass balance of antarctica, *Journal of Glaciology*, *38*, 375–386.

KOTTMEIER, C. & SELLMANN, L. 1996. Atmospheric and oceanic forcing of Weddell Sea ice motion, *Journal of Geophysical Research*, *101*, 20,809–20,824.

MELLOR, G. L. & BLUMBERG, A. F. 1985. Modeling vertical and horizontal diffusivities with the sigma coordinate system, *Monthly Weather Review*, *113*, 1379–1383.

NICOLAUS, M. & GROSFELD, K. 2002. Ice – ocean interaction underneath the Antarctic ice shelf Ekströmisen, *Polarforschung*, *72*, 17–29.

PACANOWSKI, R. C. & PHILANDER, S. G. H. 1981. Parameterization of vertical mixing in numerical models of the tropical oceans, *Journal of Physical Oceanography*, *11*, 1443–1451.

SMAGORINSKY, J. 1963. General circulation experiments with the primitive equations: I. the basic experiment, *Monthly Weather Review*, *91*, 99–164.

THOMA, M., GROSFELD, K. & LANGE, M. A. 2005a. The impact of Eastern Weddell Ice Shelves on the water masses in the eastern Weddell Sea, *Journal of Geophysical Research*, submitted.

THOMA, M., GROSFELD, K., MOHRHOLZ, C.-O. & LANGE, M. A. 2005b. Modelling ocean circulation and ice – ocean interaction in the southeastern Weddell Sea, *FRISP Report*, *16*, 33–42.

TIMMERMANN, R. & BECKMANN, A. 2004. Parameterization of vertical mixing in the Weddell Sea, *Ocean Modelling*, *6*, 83–100, doi: 10.1016/S1463-5003(02)0061-6.

TIMMERMANN, R., BECKMANN, A. & HELLMER, H. H. 2001. The role of sea ice in the fresh water budget of the Weddell Sea, *Annals of Glaciology*, *33*, 419–424.